SAND2017-10952C

Exceptional service in the national interest

Sandia National Laboratories

Opacity Modeling: Completeness, consistency, and constraints

S.B. Hansen

Sandia National Laboratories

John Castor Symposium

July 26, 2017

U.S. DEPARTMENT OF ENERGY

NNSA National Nuclear Security Administration

Sandia National Laboratories is a multimission laboratory managed and operated by National Technology and Engineering Solutions of Sandia, LLC., a wholly owned subsidiary of Honeywell International, Inc., for the U.S. Department of Energy's National Nuclear Security Administration under contract DE-NA-0003525.

Simulation- and atomic-scale models: foundations of HED

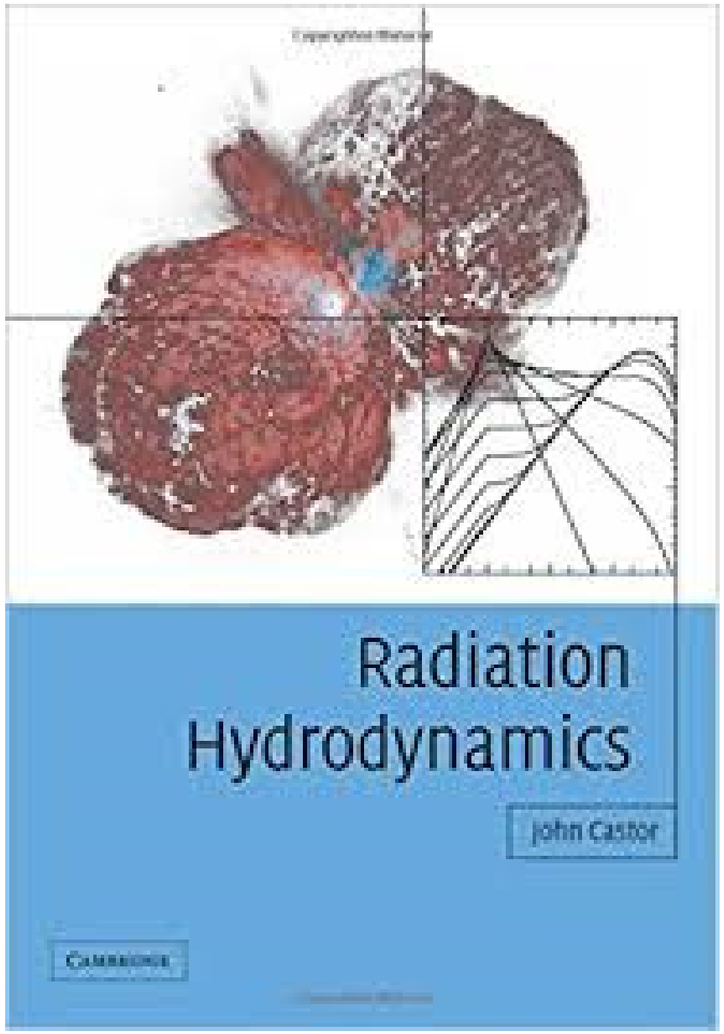

"refreshingly direct"
-- The Observatory

Radiation-hydrodynamic simulations are indispensable tools for design and diagnostics of laboratory and astrophysical HED plasmas.

Simulations rely on atomic-scale models for material properties:

- Equations of state
- Transport coefficients (electrical, thermal, stopping powers)
- Opacities and emissivities

These properties are not always consistent with each other, especially when simplifying constraints (e.g. LTE) are relaxed.

This talk will describe ongoing efforts to increase the consistency of constitutive properties used in hydro codes – and how John Castor and many others have guided these efforts along the way.

Atomic-scale constitutive models: electrons, ions, and mixtures

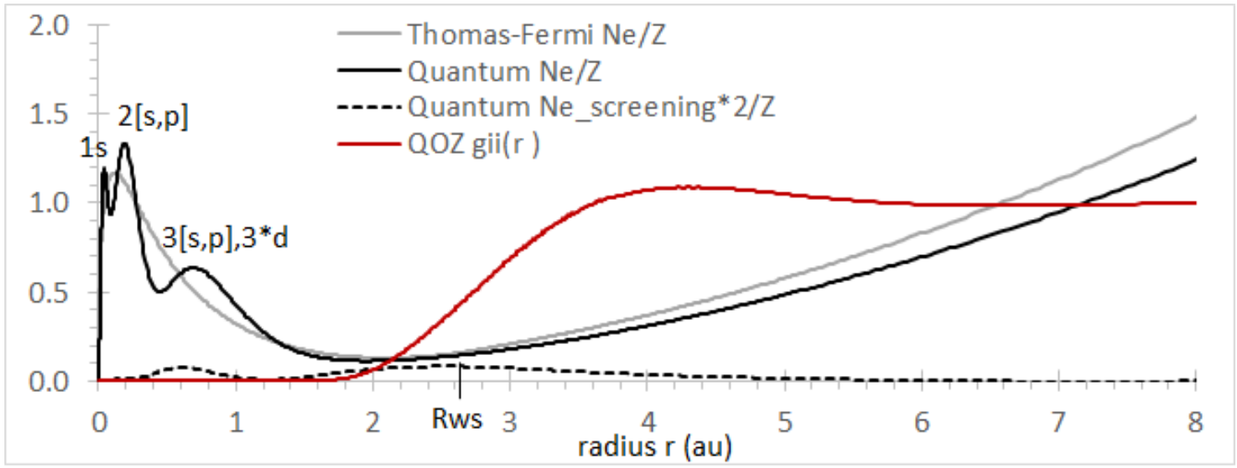

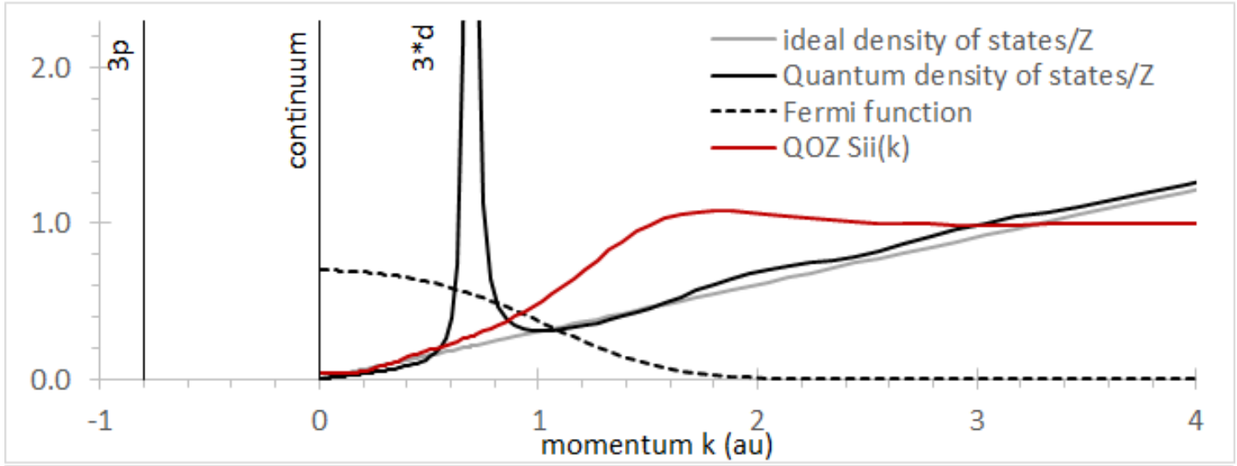

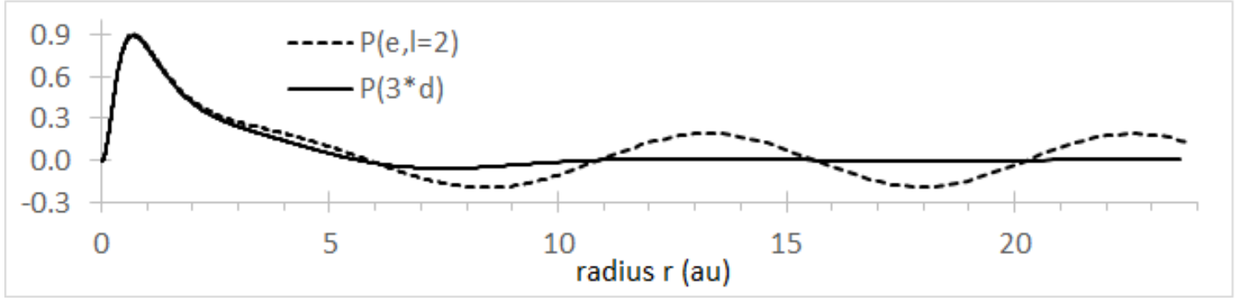

Electrons are treated quantum mechanically in a self-consistent field much like Purgatorio[1], within an ion correlation sphere instead of muffin-tin. Ions are treated with the quantum Ornstein-Zernike equations[2] using a potential generated from the self-consistent electronic structure. (Thanks, Brian, Vijay, Charlie, and Balazs!)

To ensure smooth transitions under pressure ionization, we define quasi-bound wavefunctions $P(n^*l) = \langle P(e,l) \rangle_k$ and assign them to the ion. (Thanks, Brian!)

Mixtures are treated by pressure-matching elements at fixed total density and pressure – trivial for TF, but can be tricky for quantum models. (Thanks, John and Phil!)

1. B.G. Wilson *et al*, *JQSRT* **99**, 658 (2006) 2. C. Starrett & D. Saumon, *HEDP* **10**, 35 (2014)

With self-consistent electronic and ionic structure, collisions and transport can be directly calculated

$$(\sigma_{\text{Ziman}})^{-1} = -\frac{n_i}{3\pi n_e^2}\int_0^{2k} dk\, S_{ii}(k)k^3 \int_0^{\infty} d\varepsilon \frac{df}{d\varepsilon}\frac{\partial\sigma(\varepsilon,\theta)}{\partial\theta}$$

$$\frac{\partial\sigma(\varepsilon,\theta)}{\partial\theta} = \frac{1}{p^2}\left|\sum_{l=0}^{\infty}(2l+1)\sin\eta_l e^{i\eta_l}P_l(\cos\theta)\right|^2$$

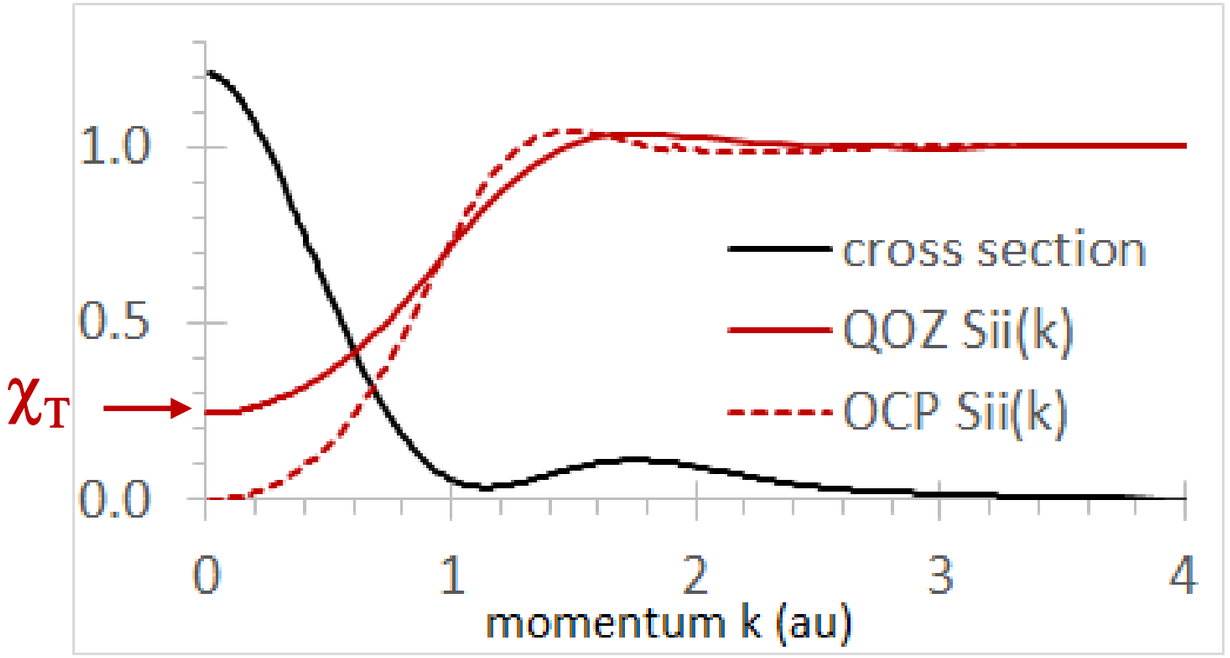

compressibility $\chi_T = T\frac{\partial\rho}{\partial p}$ should be consistent with $S_{ii}(k\rightarrow 0)$

With $S_{ii}(k)$ and phase shifts η_l from continuum states, the Ziman electrical conductivity is completely specified, offering improved consistency over treatments using ion structure factors from external sources e.g. OCP; (thanks, Hugh!).

For thermal conductivities, an additional electron-electron scattering term (not yet fully consistent within the model) is required to provide a non-Lorenz reduction factor. (thanks, John!)

For mixtures, conductivities should be volume-weighted and added in series. (thanks, John!)

Optical properties can be generated from the wavefunctions

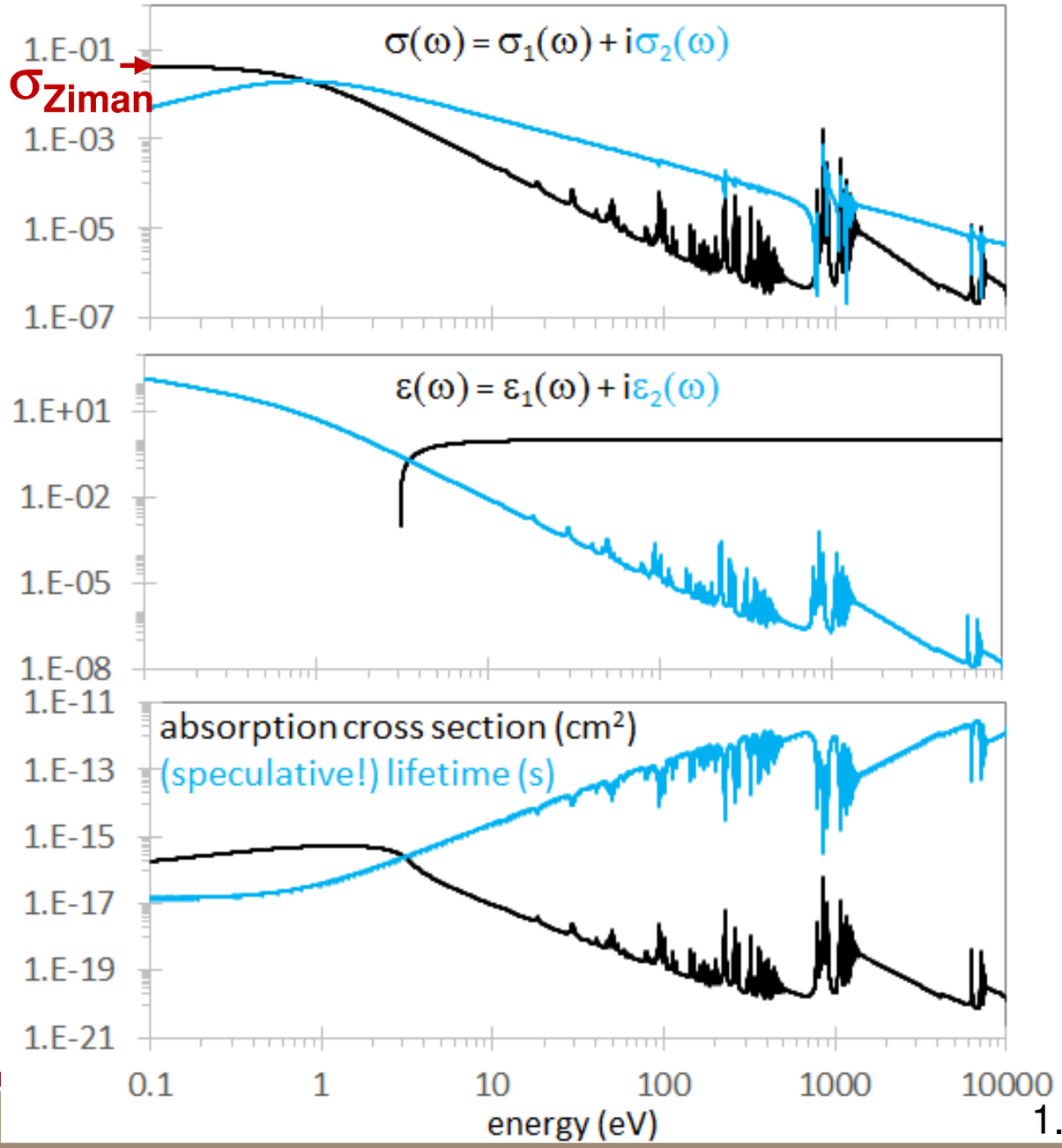

$$\sigma(\omega) = \frac{2}{3}\frac{n_a e^2}{\omega^2}\int v^3 \sigma_{tr}\left(-\frac{\partial f}{\partial E}\right)\frac{d^3p}{(2\pi\hbar)^3}$$

We use Kubo-Greenwood[1] to generate $\sigma(\omega) \rightarrow \varepsilon(\omega)$, $n(\omega)$, $\alpha(\omega)$, $\tau(\omega)$ – consistent with Ziman at $\omega = 0$ (Thanks, Walter & Joe!)

This provides crude but *strictly complete* opacities – and completeness matters! (Thanks, Carlos!) *cf.* Iglesias and Hansen, *Ap. J* **835**, 284 (2017).

We are exploring ways to increase consistency by using the optical properties to generate frequency-dependent collisional lifetimes for use in Loren**zt**ian lineshapes, using $S_{ii}(k)$ to generate P(E) for Stark splitting, and generating stopping numbers with $\varepsilon(\omega)$.

1. M. Yu Kuchiev and W.R. Johnson *et al*, *PRE* **78**, 026401 (2008)

Scattering calculations are also fully constrained

10 eV, 5 g/cc, Z_{free} = 2.6, $Z_{E>0}$ = 2.9

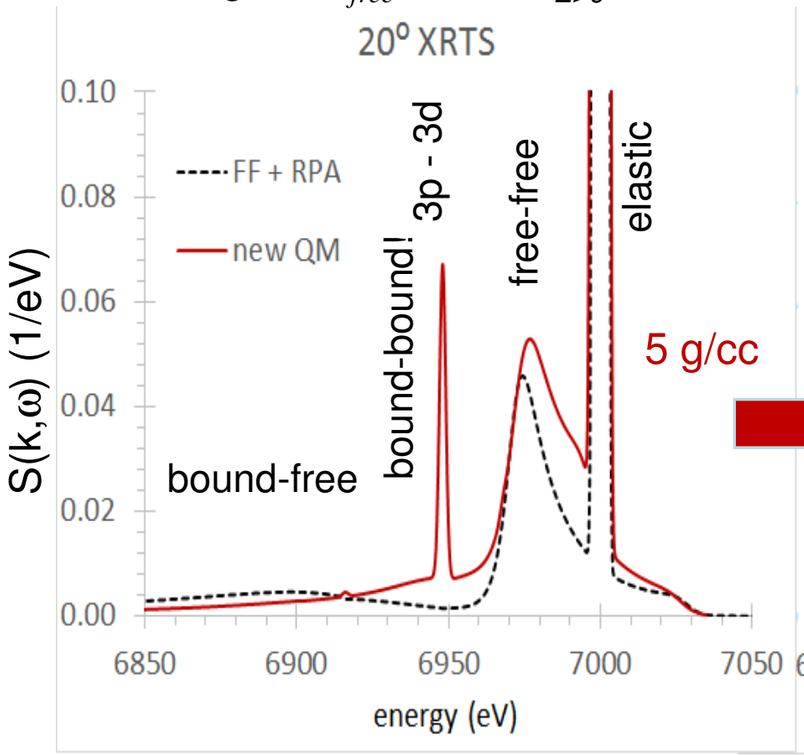

10 eV, 8 g/cc, Z_{free} = 3.2, $Z_{E>0}$ = 8.0

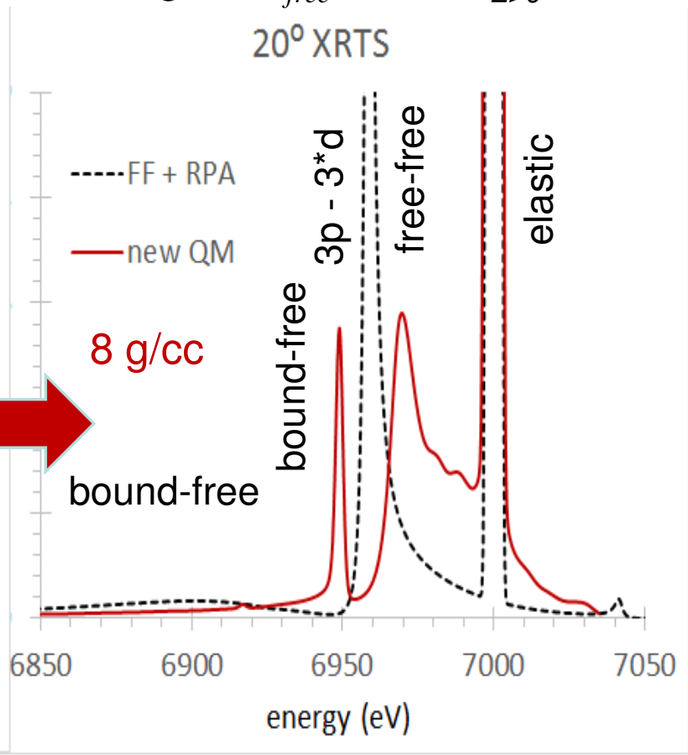

5 g/cc → 8 g/cc

$$S(k,\omega) = \underbrace{|f_I(k) + q(k)|^2 S_{ii}(k,\omega)}_{\text{elastic}} + \underbrace{\bar{Z} S_{ee}(k,\omega)}_{\text{free-free}} + \underbrace{S_{bf}(k,\omega)}_{\text{bound-free}}$$

$+ S_{bb}(k,\omega)$ (bound-bound)

Most components of the scattering signal are calculated using fully self-consistent quantities[1,2] (free-free uses RPA)

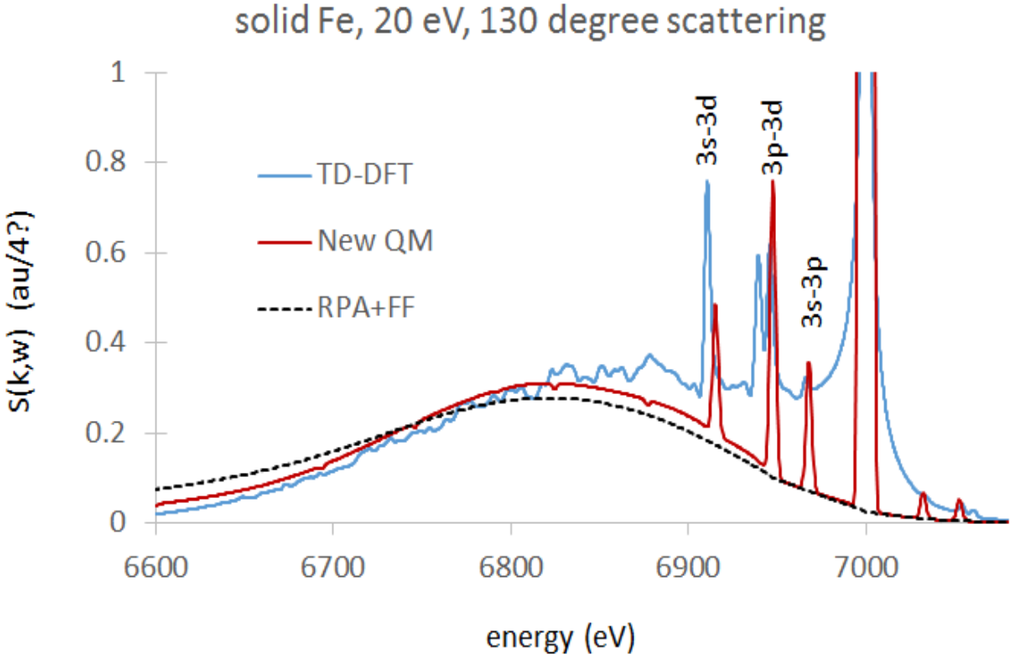

We find good agreement of the self-consistent average-atom model with time-dependent density functional theory – A. Baczewski *et al.*, PRL 116, 115004 (2016).

1. W.R. Johnson *et al*, *PRE* **86**, 036410 (2012)

2. D. Souza, C. Starrett et al., *PRE* **89**, 023108 (2014)

Consistency matters, since complex systems are susceptible to compensating errors

Sandia National Laboratories

$$(\sigma_{\text{Ziman}})^{-1} = -\frac{n_i}{3\pi n_e^2}\int_0^{2k} dk\, S_{ii}(k)k^3 \int_0^{\infty} d\varepsilon \frac{df}{d\varepsilon}\frac{\partial\sigma(\varepsilon,\theta)}{\partial\theta}$$

$$\frac{\partial\sigma(\varepsilon,\theta)}{\partial\theta} = \frac{1}{p^2}\left|\sum_{l=0}^{\infty}(2l+1)\sin\eta_l e^{i\eta_l}P_l(\cos\theta)\right|^2$$

$$\sigma(\omega) = \frac{2}{3}\frac{n_a e^2}{\omega^2}\int v^3\sigma_{\text{tr}}\left(-\frac{\partial f}{\partial E}\right)\frac{d^3p}{(2\pi\hbar)^3}$$

$$S_{bf}(k,\omega) = \sum_{n\ell}\frac{4(2\ell+1)p}{\pi}\mathcal{F}(\epsilon_{n\ell})(1-\mathcal{F}(\epsilon))M(\epsilon_{n\ell})$$

$$\times\sum_{\ell_1\ell_2}A_{\ell_1\ell\ell_2}\left|I_{\ell_1\ell\ell_2}(p,k)\right|^2$$

$$I_{\ell_1\ell\ell_2}(p,k) = \frac{1}{p}\int_0^{\infty}P_{\epsilon\ell_1}(r)j_{\ell_2}(kr)P_{n\ell}(r)\sqrt{f^{\text{cut}}(r)}dr,$$

$$\left(\frac{dE}{dx}\right) = -\frac{4\pi}{m}\left(\frac{Ze^2}{V}\right)^2\int_0^{\infty}\rho(r)L(\rho,V)4\pi r^2 dr$$

$$L(\rho,V) = \frac{i}{\pi\omega_0^2}\int_0^{\infty}\frac{dk}{k}\int_{-kV}^{kV}\omega dw\left(\frac{1}{\varepsilon(k,\omega)}-1\right)$$

The complexity of expressions for transport, scattering, and stopping tempts us to simplify wherever we can.

However, unless consistency is enforced among the model parts, we run a real risk of generating hidden compensating errors when fitting to (sparse!) data: we risk being "right" for the wrong reasons (thanks, Andrew!)

If the present model is wrong, it will be *consistently* (and hopefully obviously) wrong. And because its predictions are interdependent, measurement of one property can help constrain others.

Completeness matters as well, and can be challenging to achieve with highly detailed opacity models

Sandia National Laboratories

Computational costs vary dramatically, and adequate inline non-LTE models have only recently become available (Thanks, Howard!)

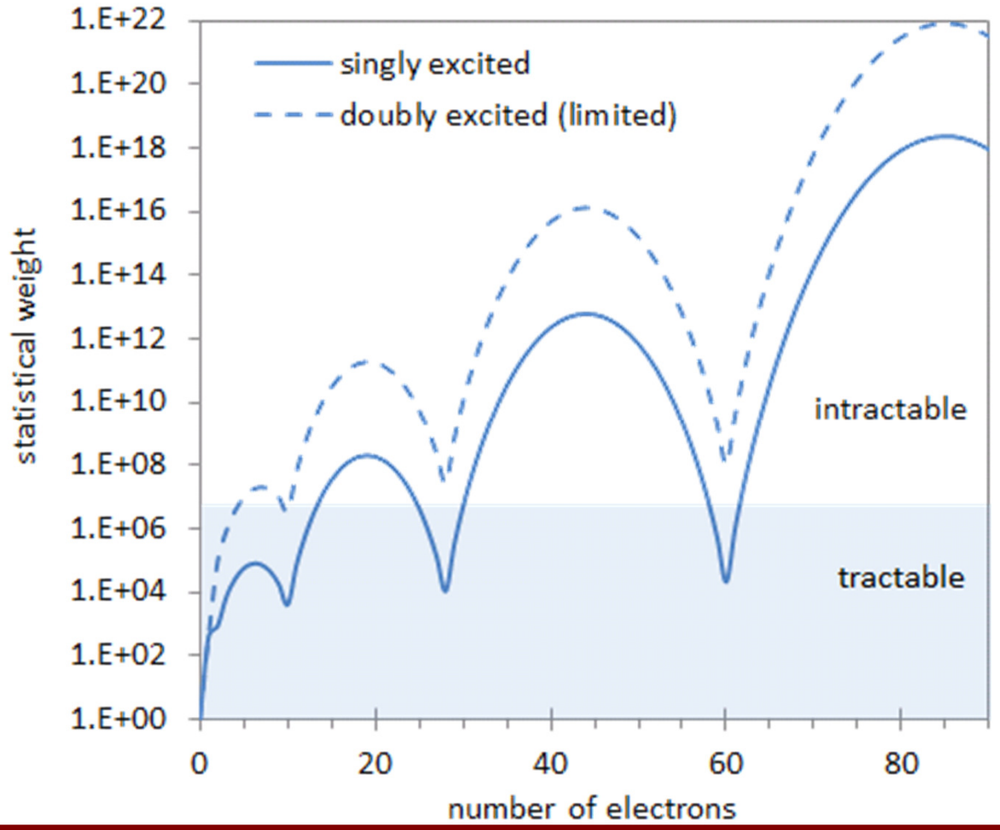

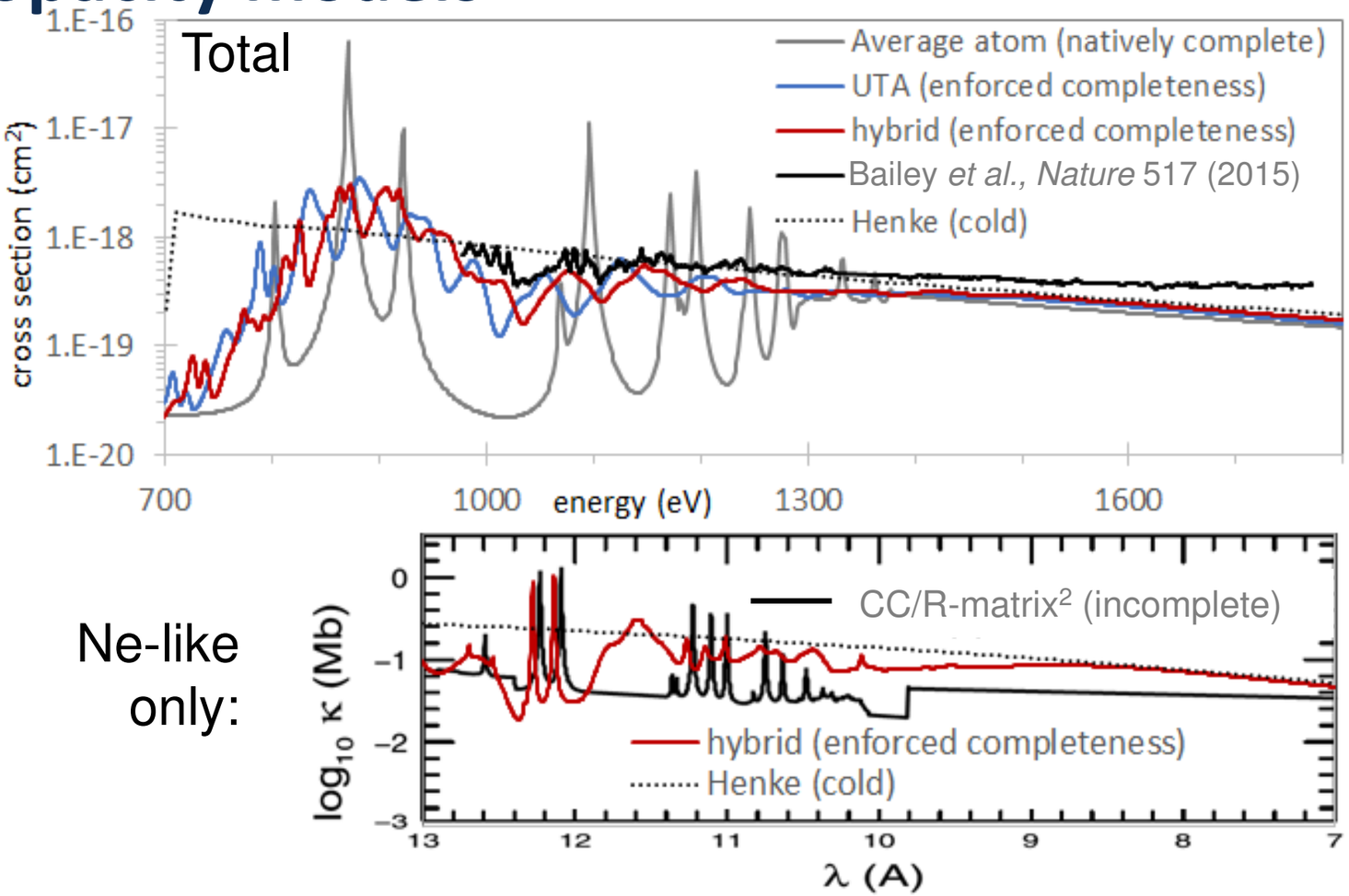

Ne-like only:

While sufficient detail is important for comparisons with experiment, completeness is a first-order requirement.[3]

1. HA Scott & SBH, HEDP **6**, 39 (2010) 2. Nahar and Pradhan, PRL **116** (2016) 3. CA Iglesias & SBH, *Ap. J* **835**, (2017).

Can a consistent and complete model help address the iron opacity puzzle?

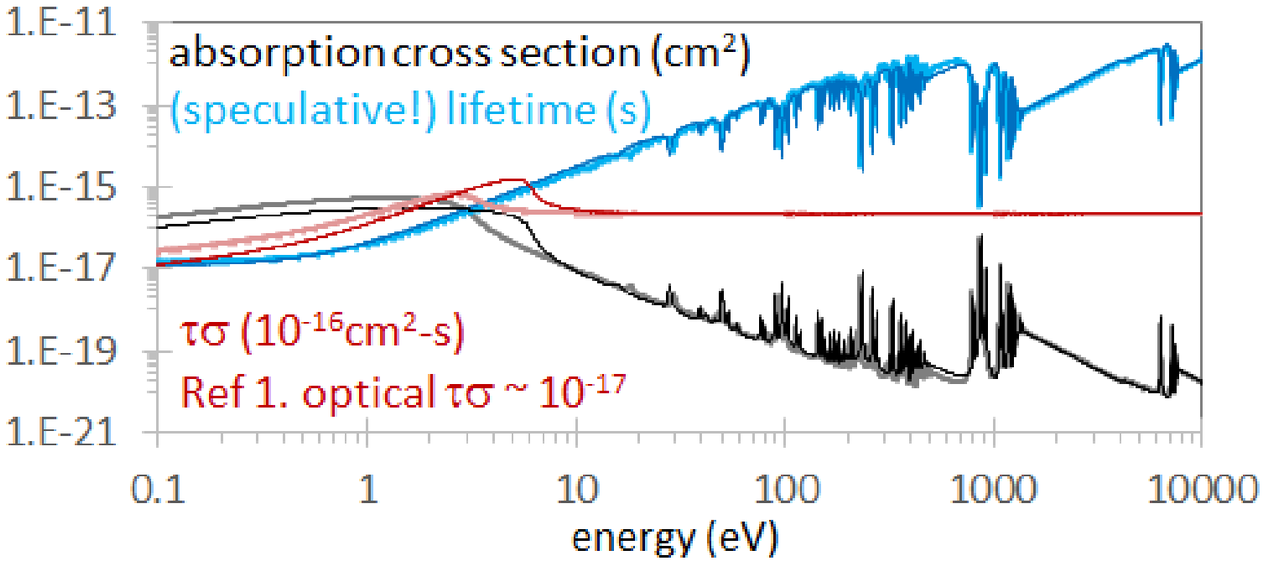

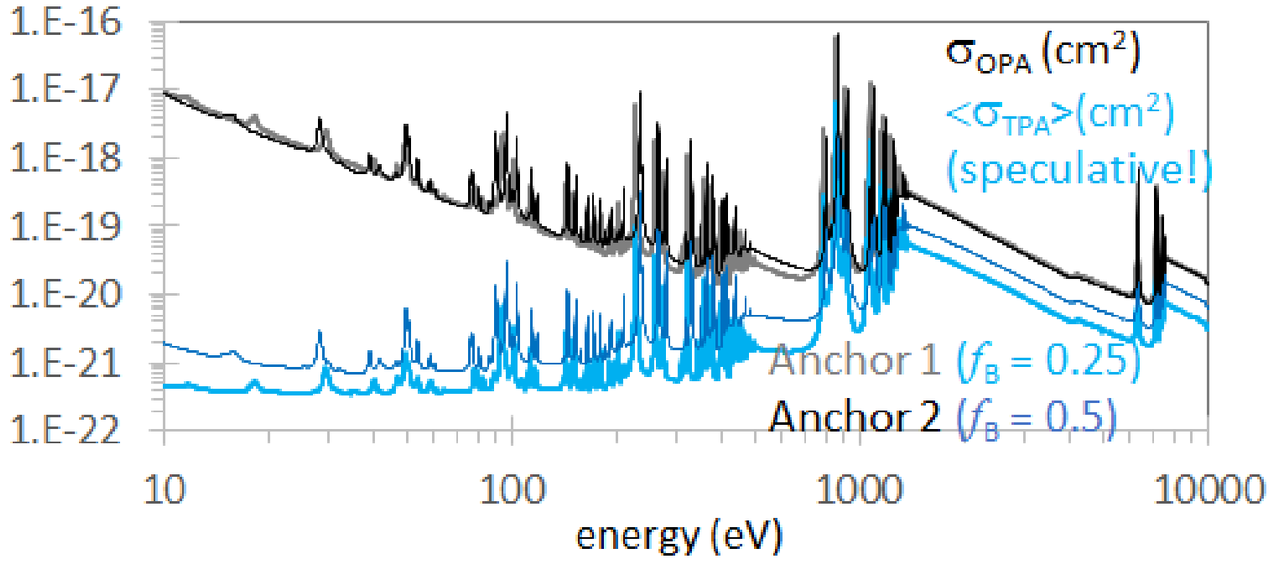

High-precision measurements (Bailey *et al.*, *PRL* **99**, 265002 (2007) and *Nature* **517**, 56 (2015)) showed good agreement with detailed models at 150 eV, $n_e = 8\times10^{21}$ e/cc but profound disagreement at 180 eV, $n_e = 3\times10^{22}$ e/cc.

Following Lambropolous & Tang [1], we take

$\sigma_{TPA} = \sigma_{i\text{-}j}\ \tau_j\ \sigma_{j\text{-}f}$ [cm^4 s]

$\langle\sigma_{TPA}\rangle = \sigma_{OPA} \int_0^Q (\tau_j\ \sigma_{j\text{-}f})(\omega)\ f_B\, B(\omega)\ d\omega$ [cm^2]

with $f_B\, B(\omega)$ the backlighter photon flux and

$\tau(\omega) = n_i / [\varepsilon_2(\omega)d\omega]$ **(?, from [2])**

Please note, this is highly preliminary; see recent work from R. More and M. Kruze for more rigorous approaches.
(Thanks, Richard!)

1. Lambropolous & Tang, *J. Opt. Soc. Am. B* **4**, 821 (1987) 2. F. Wooten, Optical Properties of Solids, NY Ac.Press Eq. 3.108

As we push material to increasingly extreme conditions, density effects become significant

High-resolution spectra from MagLIF plasma (E. Harding)

Liner is Be with ~200 ppm Fe

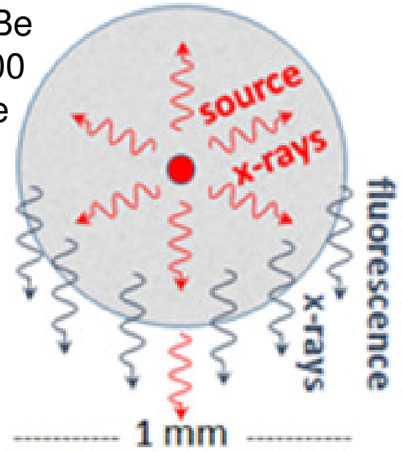

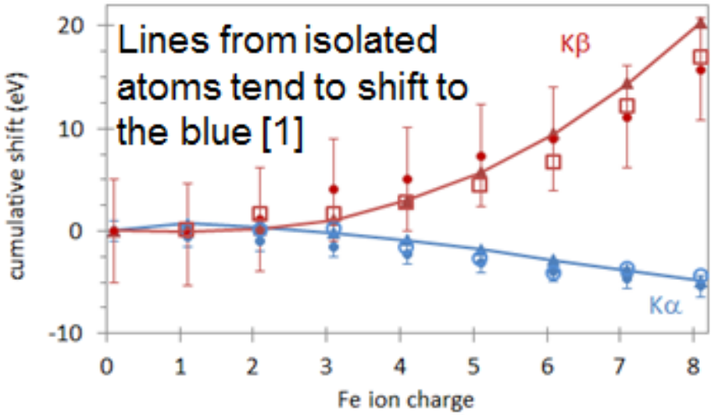

(Thanks, Brian!)

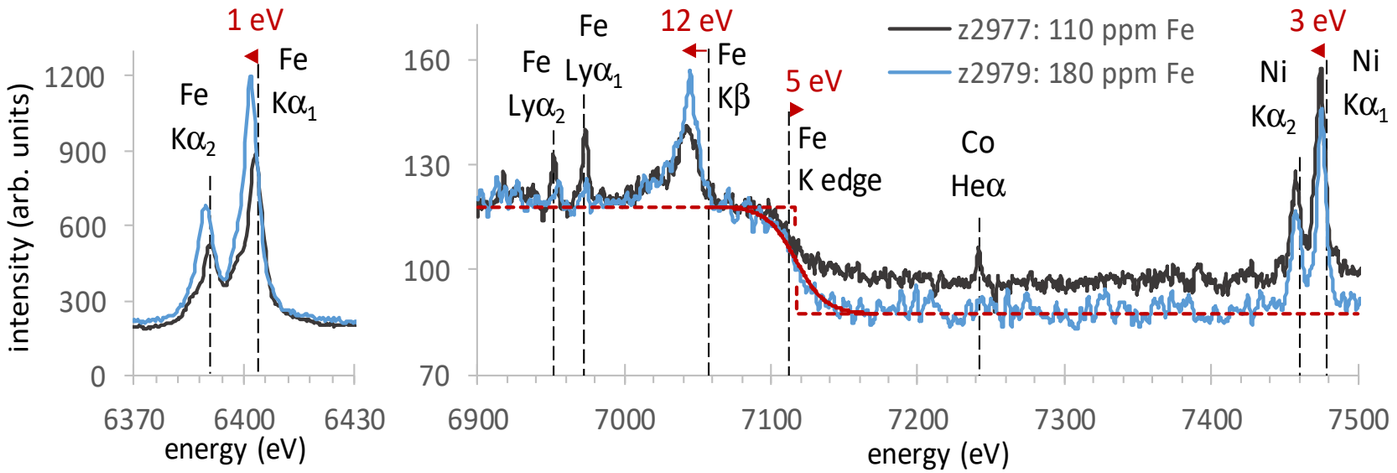

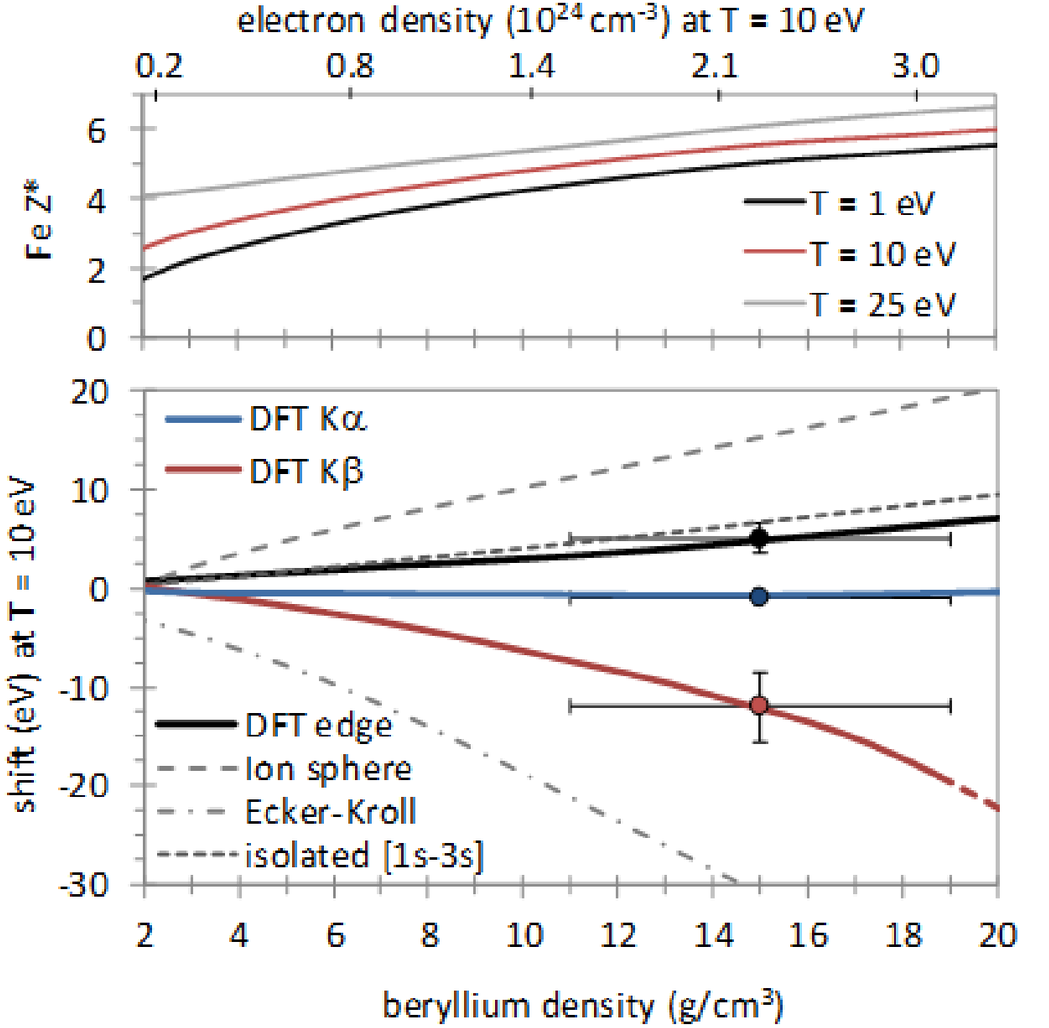

Fe Kβ lines in highly compressed material undergo red shifts, while the Fe K-edge is relatively stable.

1. D.A. Liberman, J.R. Albritton, B.G. Wilson, and W.E. Alley, Phys. Rev. A **50**, 171 (1994).

Conclusions

Sandia National Laboratories

- Enforcing consistency in atomic-scale model predictions for multiple material properties can increase confidence in both diagnostics and simulations of HED plasmas.
  - Scattering, emissivity and opacity (including two-photon processes)
  - Collisionality and transport (thermal, electrical, and stopping powers)
  - Coupled electronic and ionic structure (Equations of State)

- If the present model is wrong, it will at least be *consistently* wrong –
  and its wrongness can be determined by measurement[s] of inter-dependent observables.

- The rich and collaborative scientific environment at LLNL offers researchers amazing opportunities to develop and apply their own contributions to HED science…

Conclusions

Sandia National Laboratories

- Enforcing consistency in atomic-scale model predictions for multiple material properties can increase confidence in both diagnostics and simulations of HED plasmas.
  - Scattering, emissivity and opacity (including two-photon processes)
  - Collisionality and transport (thermal, electrical, and stopping powers)
  - Coupled electronic and ionic structure (Equations of State)

- If the present model is wrong, it will at least be *consistently* wrong –
  and its wrongness can be determined by measurement[s] of inter-dependent observables.

- The rich and collaborative scientific environment at LLNL offers researchers amazing opportunities to develop and apply their own contributions to HED science…

Thanks, John! (and many, many others!)

Electronic boundary conditions influence EOS

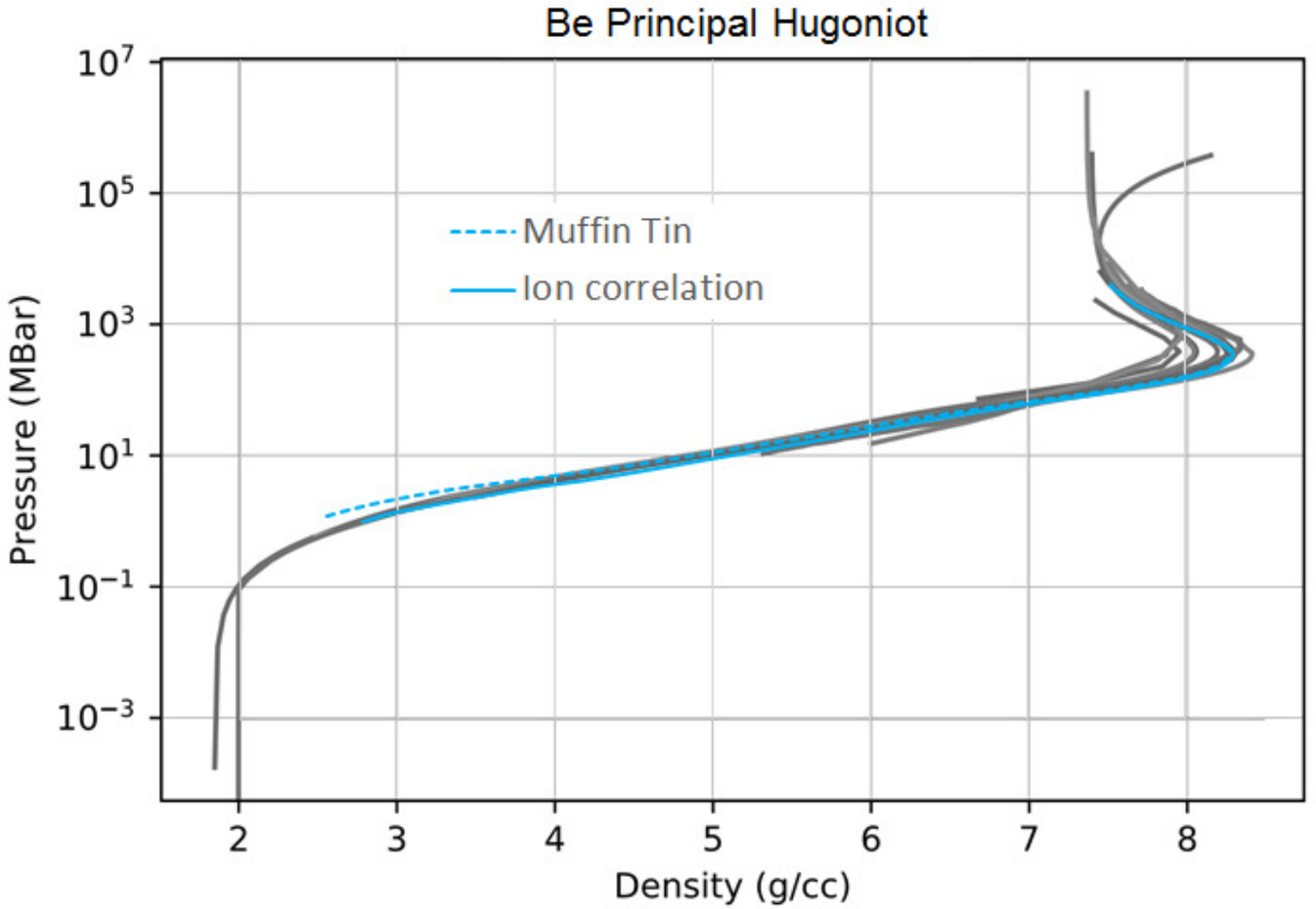

These curves use ideal-gas behavior for ions and so reveal differences between electronic boundary conditions in IS & NPA models; the NPA consistency can be improved.

Be Hugoniots courtesy J. Gaffney & Suxing Hu, from 2017 EOS code comparison workshop

Stopping Powers are calculated following Wang et al. (cf. Faussurier) using data fro

Stopping power is the integral of stopping number L(ρ,V) over average-atom electron density ρ(r):

$$\left(\frac{dE}{dx}\right) = -\frac{4\pi}{m}\left(\frac{Ze^2}{V}\right)^2 \int_0^\infty \rho(r) L(\rho,V) 4\pi r^2 dr$$

The stopping number is related to the dielectric -- currently using RPA L(ρ,V) from Arista & Piriz, PRA 35, 3450 (1987)

$$L(\rho,V) = \frac{i}{\pi\omega_0^2}\int_0^\infty \frac{dk}{k}\int_{-kV}^{kV} \omega dw \left(\frac{1}{\varepsilon(k,\omega)} - 1\right)$$

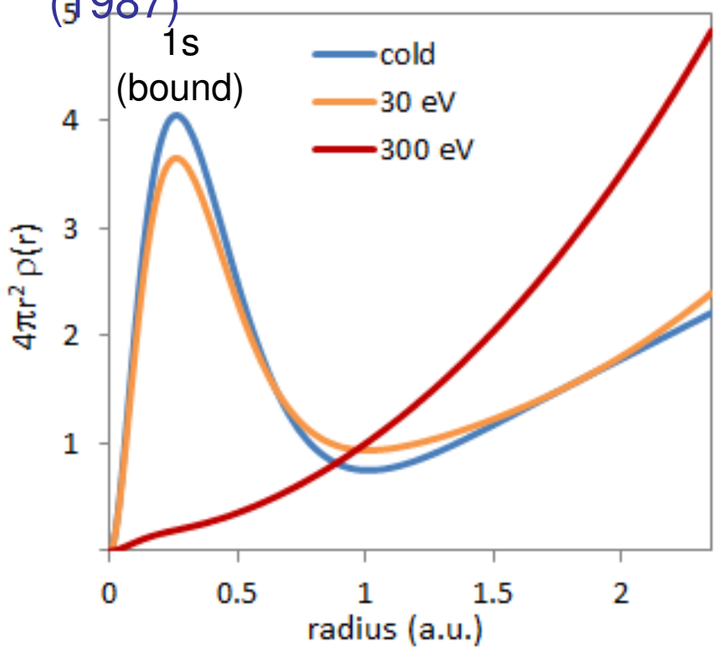

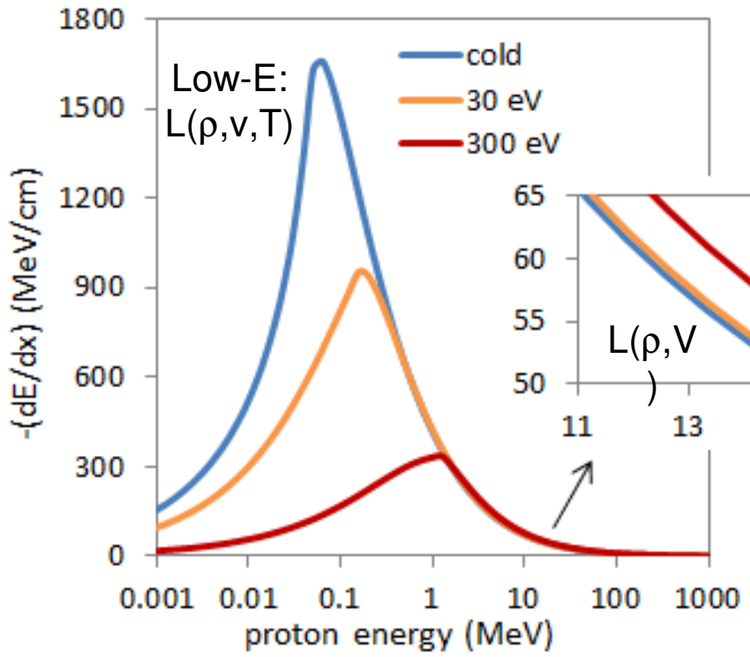

In the high-energy (Bethe) limit, L(ρ,v) is independent of T → dE/dx increases with Z*

Calculations are for solid-density Be

These all-electron calculations take about a minute for a single ρ,T point

*Wang, et al., Phys Plas 5, 2977 (1998); Faussurier et al., Phys Plas 17, 052707 (2010)

These calculations (AA-LDA) described Zylstra's recent measurements of 14 MeV proton stopping reasonably well

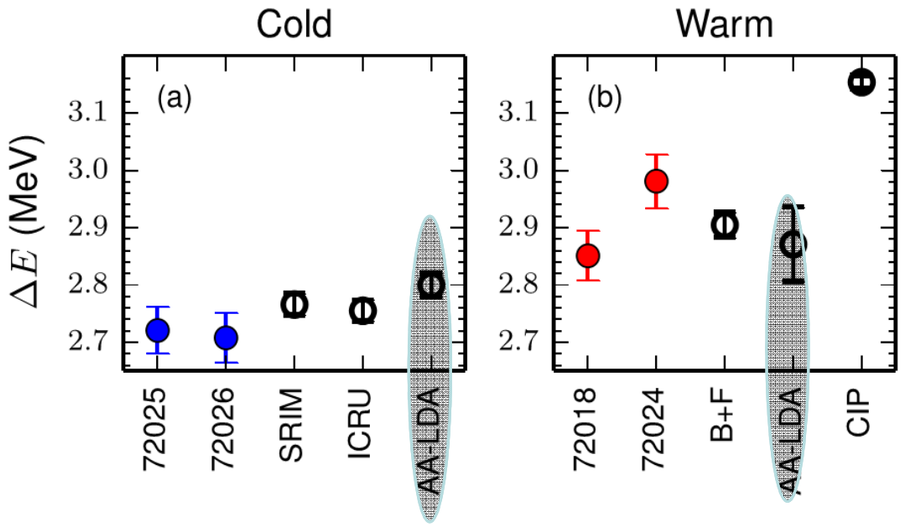

FIG. 4 (color online). Downshift (ΔE) for cold (a) and warm (b) shots compared to theory. The solid points are data (denoted by shot number), and theories are hollow points. The uncertainties in theoretical calculations are due to uncertainties in ρL and plasma conditions.

The downshift of 14 MeV protons is determined by integrating calculated dE/dx over measured path length

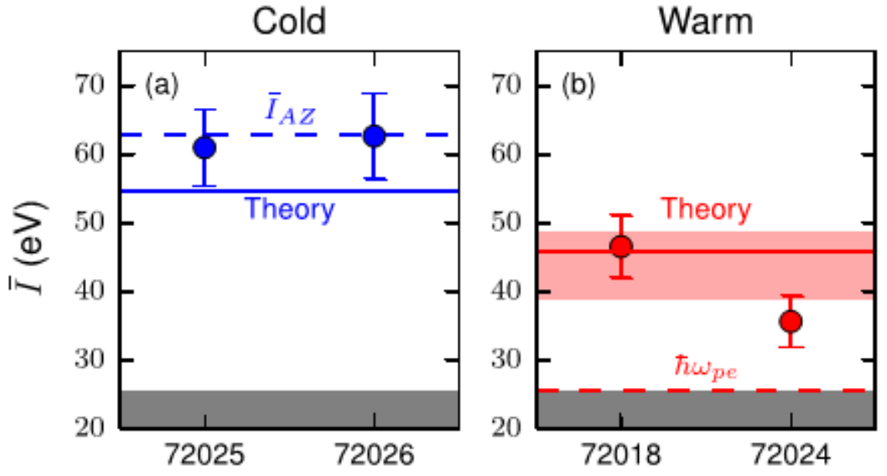

FIG. 5 (color online). Mean ionization potential ($\bar{I}$) inferred from the stopping-power data in the cold (a) and warm (b) cases compared to the Andersen-Ziegler empirical fits ($\bar{I}_{AZ}$), the ideal plasma case ($\hbar\omega_{pe}$), and electronic structure theory.

Mean ionization potential can be calculated simply by averaging $E_{binding}$ + E_{Fermi} for all electrons in the Average Atom calculation

From Zylstra et al., Phys Rev Lett 114, 215002 (2015)

Electrons: Quantum mechanical average atom

All-electron, fully quantum-mechanical* semi-relativistic self-consistent field solver with flexible exchange

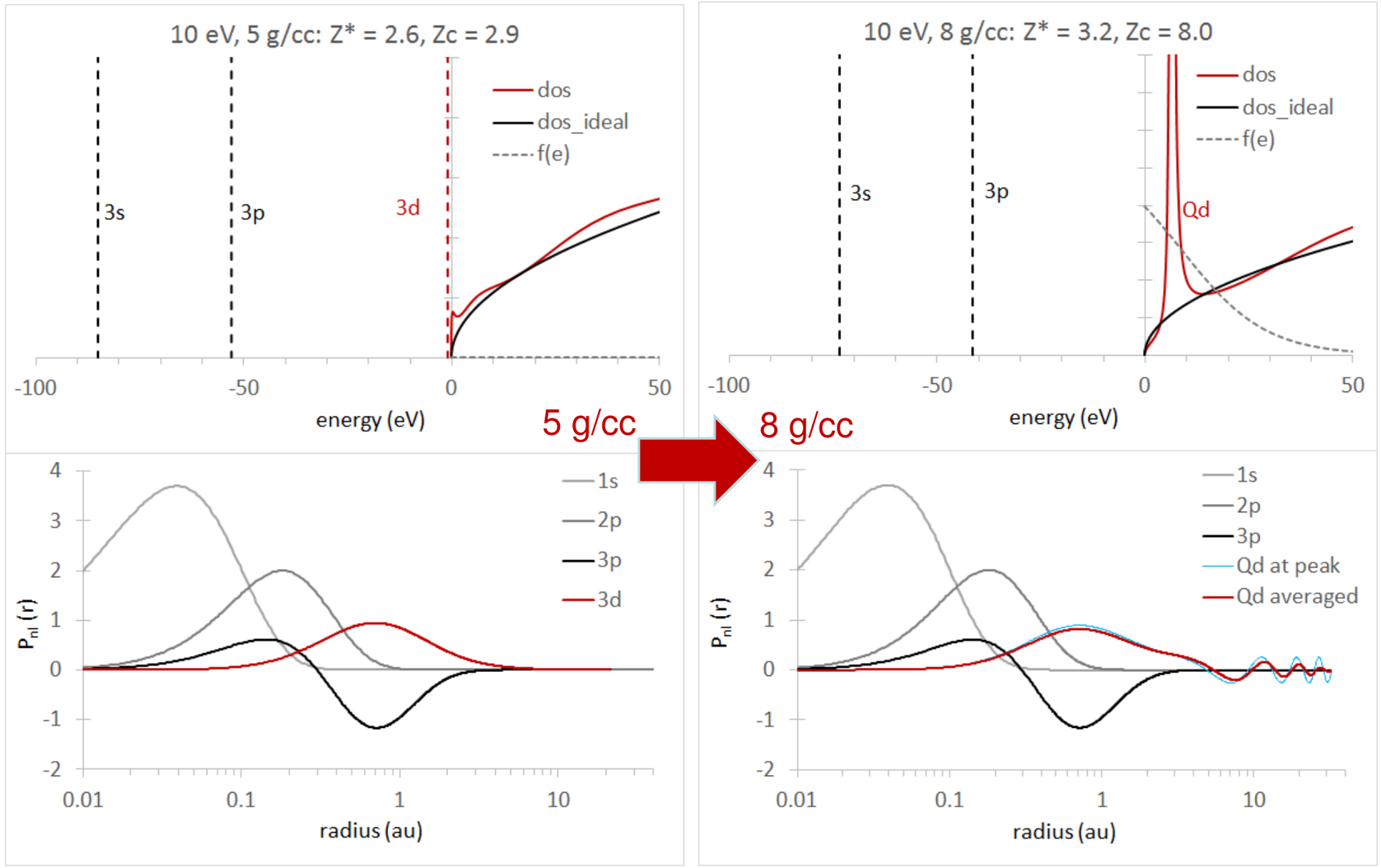

Near-solid iron at T = 10 eV

Key ansatz:
Quasi-bound states are averaged over resonance features in the DOS and treated *just like* bound states

This ensures smooth variation of constitutive & observable properties under pressure ionization – and collapses multiple definitions of Z* into a single value [*cf.* Murillo *et al.*, *PRE* **87**, 063113 (2013)]:

$$
\begin{aligned}
Z^* &= \int d\varepsilon\, f(\mu,\varepsilon) DOS_{ideal} && (Z_{free})\\
&= \int \rho_{scr}\, dr = \tilde{V}_{ie}(k=0) && (Z_{scr})\\
&= \int d\varepsilon\, f(\mu,\varepsilon)(1-f(\mu,\varepsilon))\varepsilon^{3/2} && (Z_{Boltz})\\
&= \tfrac{1}{3}(R^3_{WS}/R^2_{max})\rho(R_{max}) && (Z_{asymp})\\
&\approx \tfrac{1}{3} R_{WS}\, \rho(R_{WS}) && (Z_{WS})\\
&\neq \int d\varepsilon\, f(\mu,\varepsilon)\ DOS = Z_n - Z_b && (Z_{\varepsilon>0})
\end{aligned}
$$

*D. A. Liberman, *Phys. Rev. B* **20**, 4981 (1979), B.G. Wilson *et al*, *JQSRT* **99**, 658 (2006)

Ions: Quantum Ornstein-Zernike

Self-consistent V_{ii} & g_{ii} obtained by finding electron density with (ρ^{tot}) and without (ρ^{ext}) central charge*

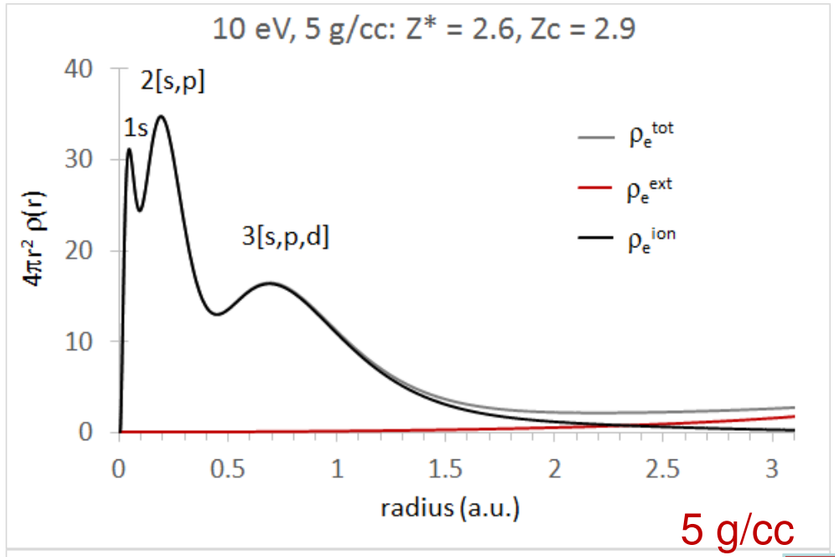

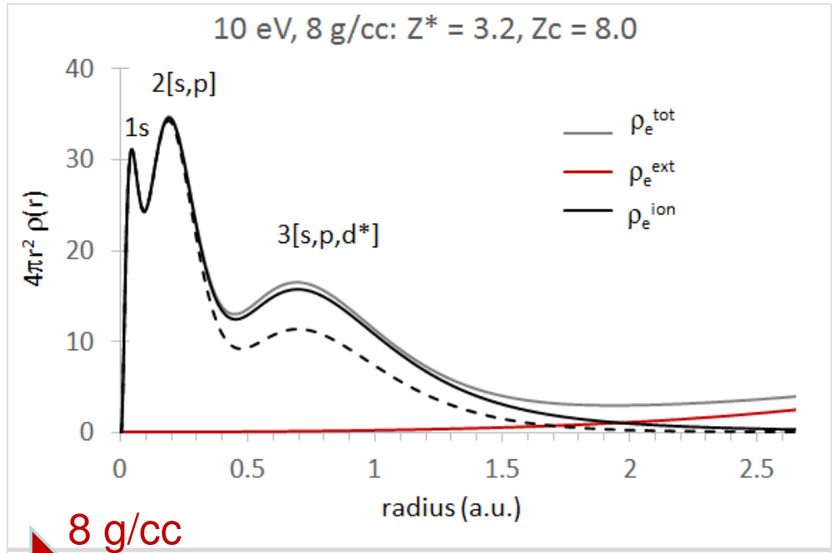

5 g/cc → 8 g/cc

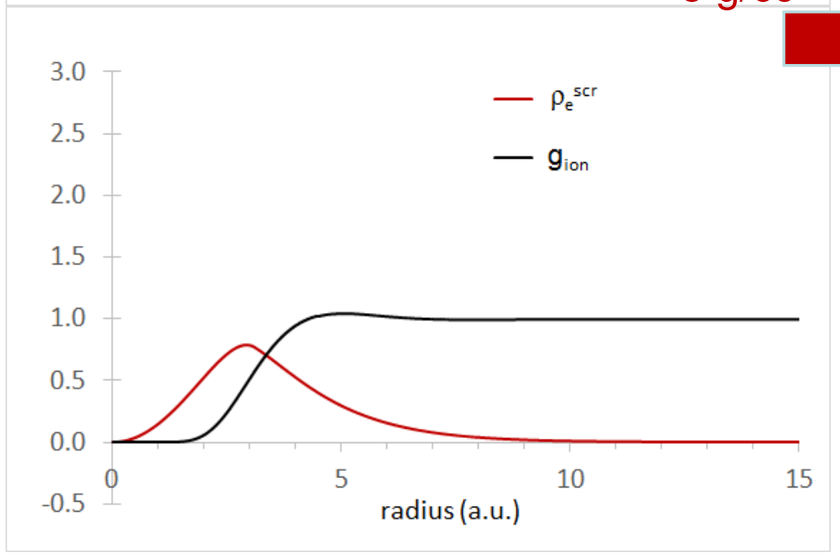

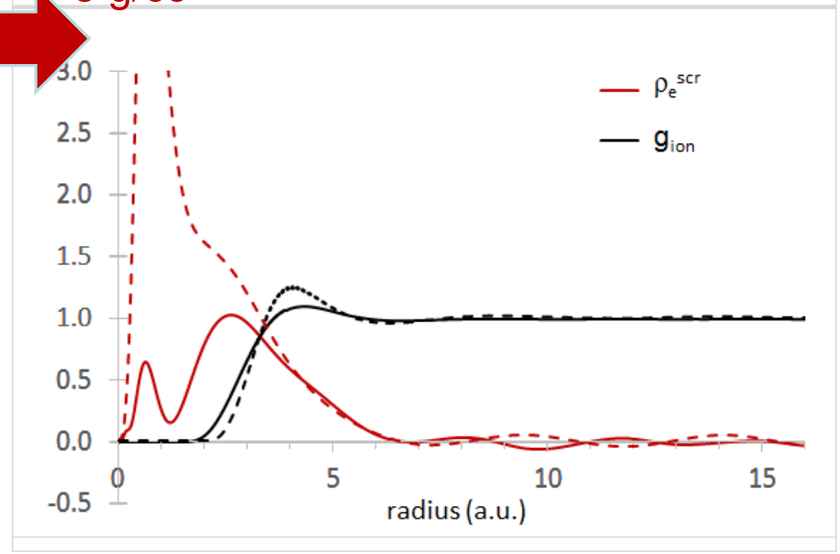

$\rho^{PA} = \rho^{tot} - \rho^{ext}$
$\rho^{scr} = \rho^{PA} - \rho^{ion}$

Like Z*, ρ^{ion} is not uniquely defined

New ansatz (solid): $\rho^{ion} = \rho^{b} + \rho^{q\text{-}b}$
Standard (dashed): $\rho^{ion} \approx \rho^{b}$

The new ansatz leads to smaller changes in screening under pressure ionization and softer g(r)

Combined with smooth changes in Z*, this leads to smooth variations in model predictions for both constitutive properties and experimental observables

*C. Dharma-Wardana & F. Perrot, *Phys. Rev. E* **26**, 2096 (1982), C. Starrett & D. Saumon, *HEDP* **10**, 35 (2014)

Constitutive properties: static and dynamic conductivities

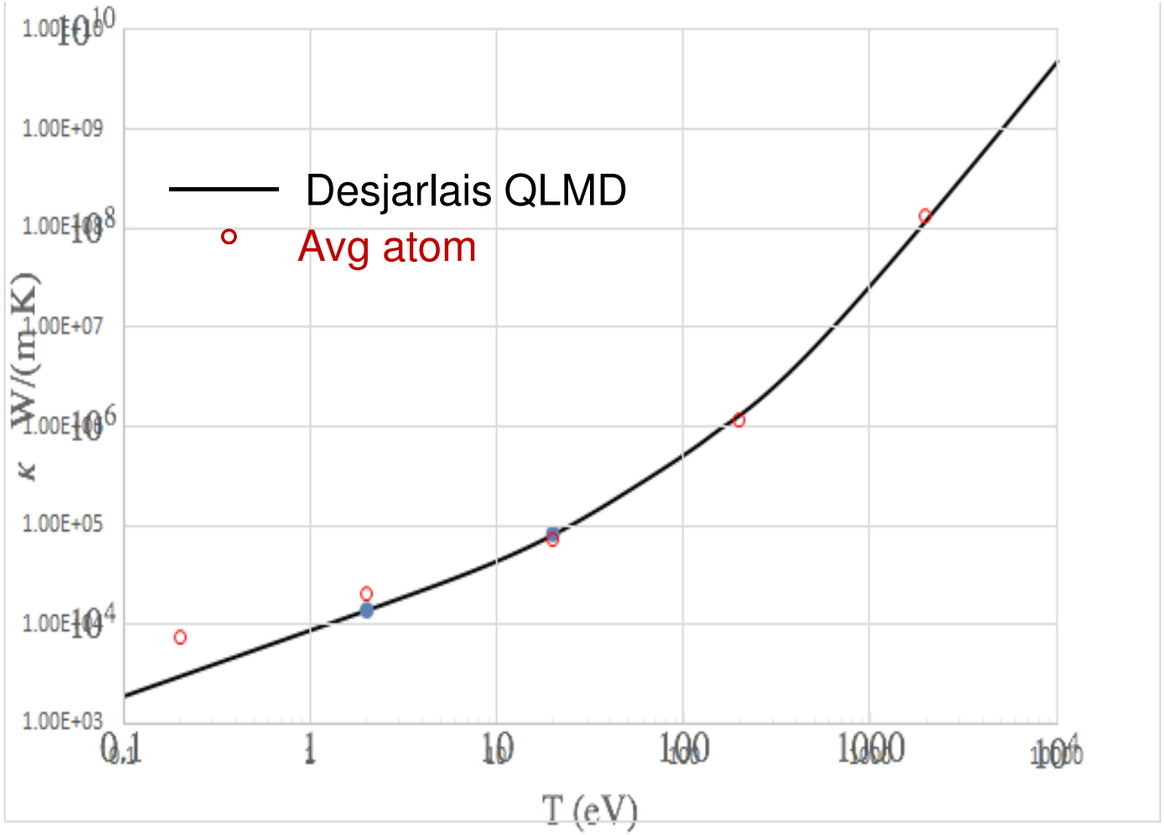

We find fair agreement with DFT-MD static electrical and ee-corrected thermal conductivities of 10 g/cc hydrogen, though the ω = 0 limit can be tricky [Burrill and Starrett, HEDP 19, 1 (2016).]

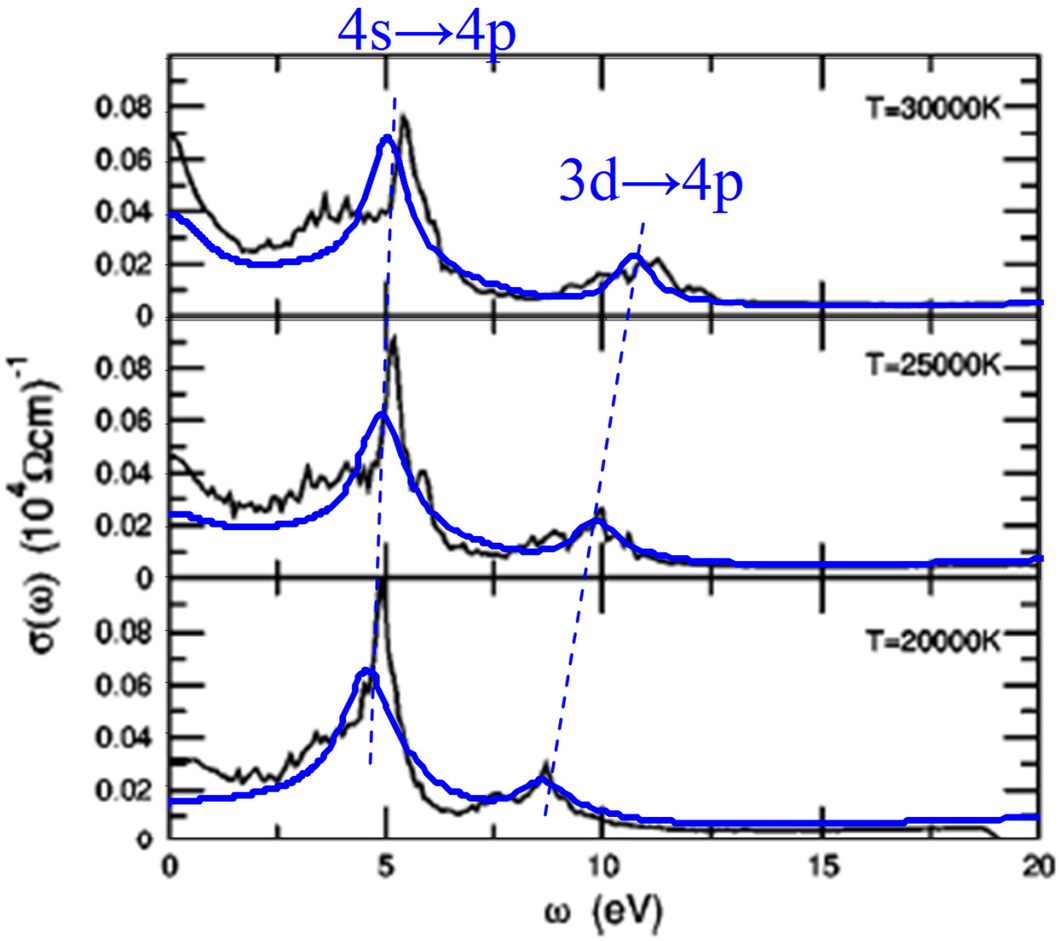

We find favorable agreement with DFT-MD calculations* of Cu σ(ω) at 0.5 g/cc and T = 1 - 3 eV. Here, the optical lines shift to higher energy as the average ion charge increases.

*Clerouin et al, Phys. Rev. B 71, 064203 (2005).

Fe K-edge shape and depth roughly constrain liner conditions

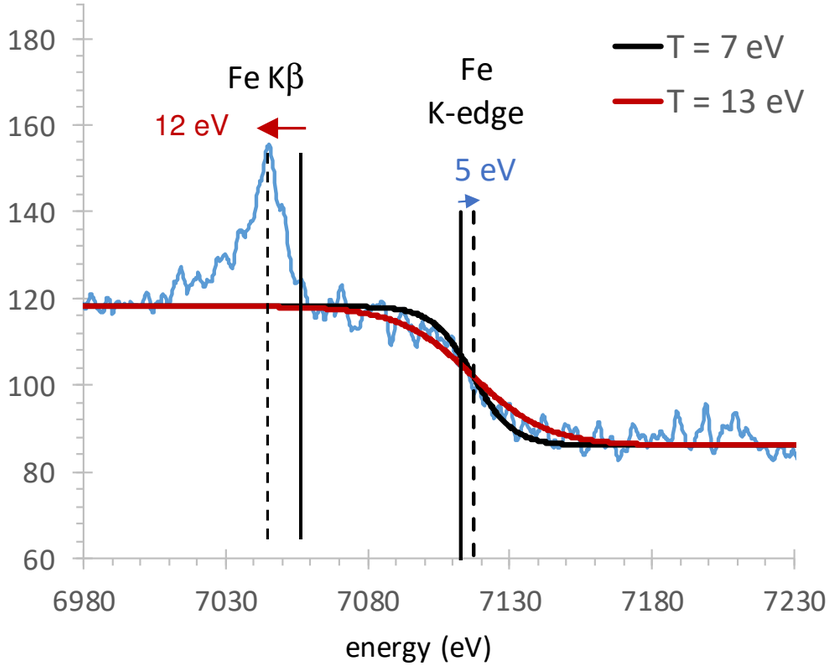

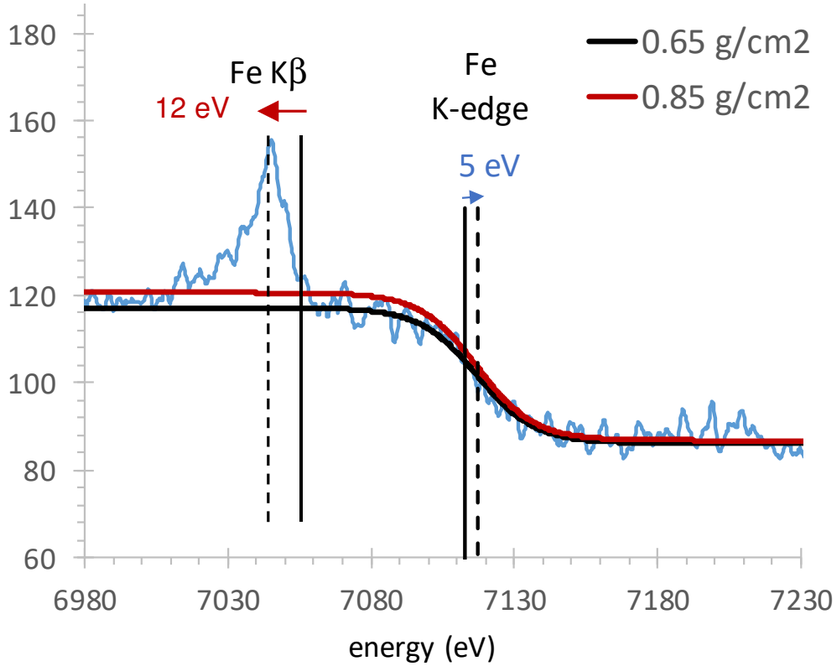

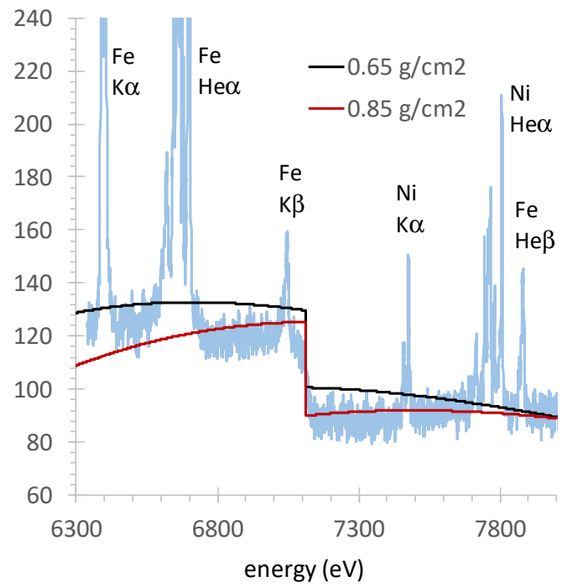

The temperature broadening of the Fermi distribution feeds into shape of the K-edge absorption and is independent of density for $T < E_{Fermi}/4$*

For this lineout, **T = 10 +/- 3 eV** and the edge exhibits a modest shift of +5 eV from cold iron. (If there are other sources of broadening, T ~ 10 eV may be an upper limit.)

With known Fe impurity concentration, the K-edge depth constrains ρR and is independent of temperature for T < 1 keV. Here, ρR = 0.75 +/- 0.1 g/cm^2

Since ρR increases monotonically with compression, we can infer a uniform liner density **ρ = 15 +/- 5 g/cm^3** (n_e ~ 2 x10^{24} e/cc), assuming no axial redistribution or mass loss and final inner liner radius of 50 μm.

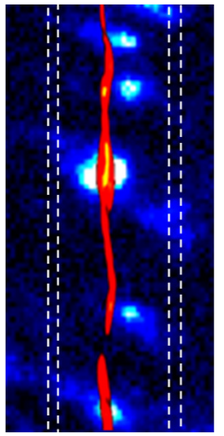

The ρR inferred from the Fe K-edge depth is consistent with ρR inferred from bulk Be absorption and low-energy self-emission images

*F. Dorchies *et al,* PRB **92**, 085117 (2015)

Observables in extreme WDM: absorption edges and fluorescence lines

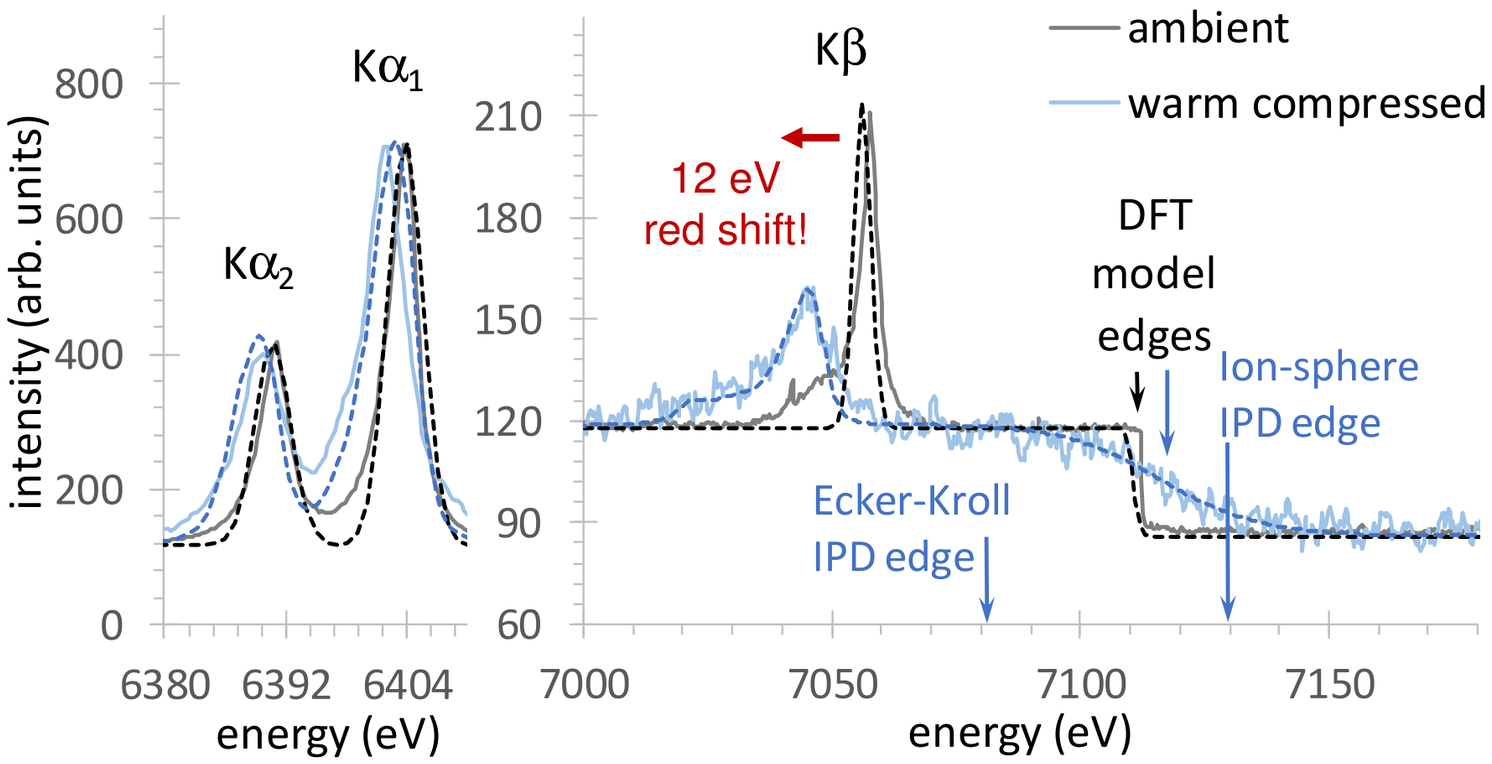

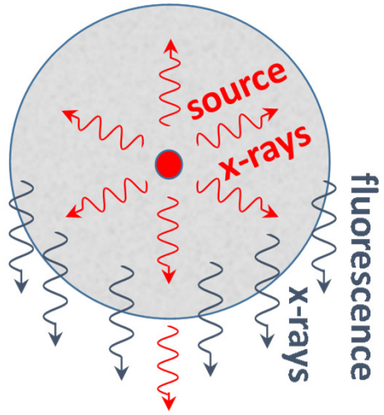

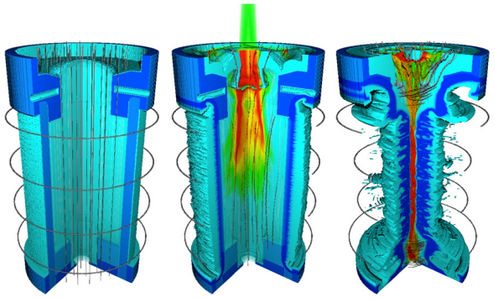

Calculations (dashed lines) anchored to the K-edge of ambient data (solid gray) show good agreement with line and edge shifts and broadening due from a warm compressed MagLIF liner backlit by stagnation emission (solid blue) with T ~ 10 eV and n_e ~ $2x10^{24}$ e/cc.

This agreement indicates that self-consistent DFT models describe electronic structure in extreme conditions with better fidelity than ad-hoc models of density effects.

*Hansen et al, submitted

We are pursing additional efforts to assess uncertainties in the constituent models used in hydro codes

Sandia National Laboratories

A first transport code comparison workshop was held at SNL in October 2016
40 attendees and 20 codes representing MD, DFT-MD, AA/NPA DFT, and analytic approaches contributed Z*, κ, σ, ν, d, dE/dx… for H, C, and CH at degenerate to classical conditions

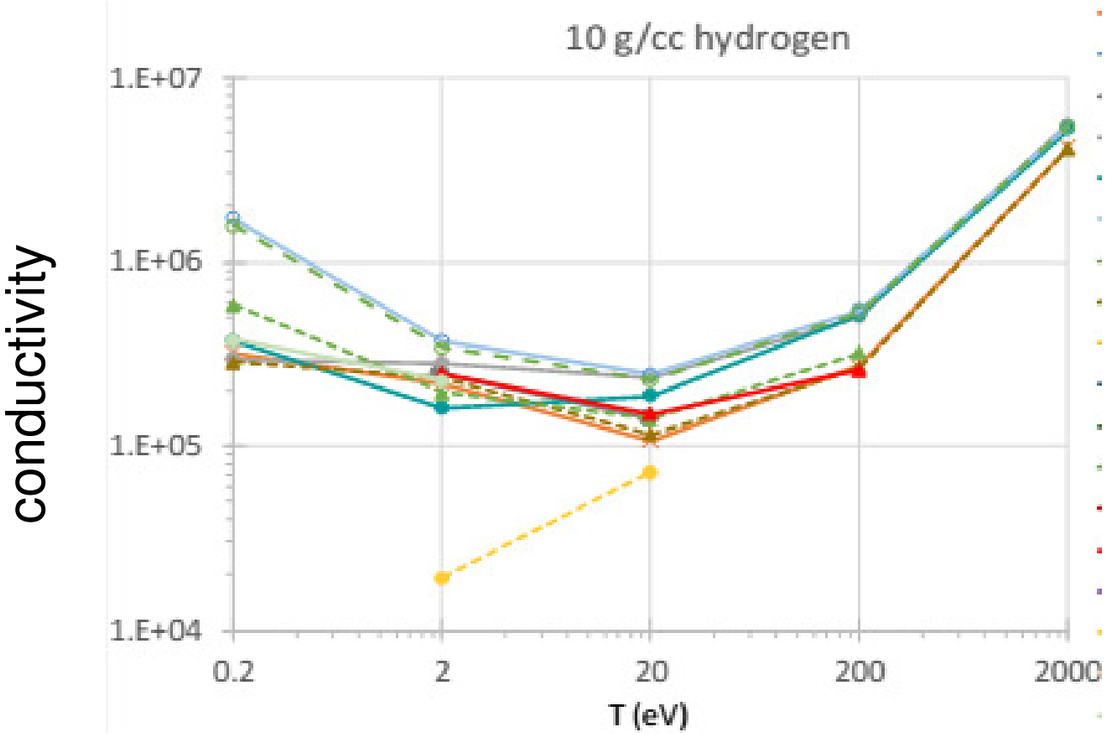

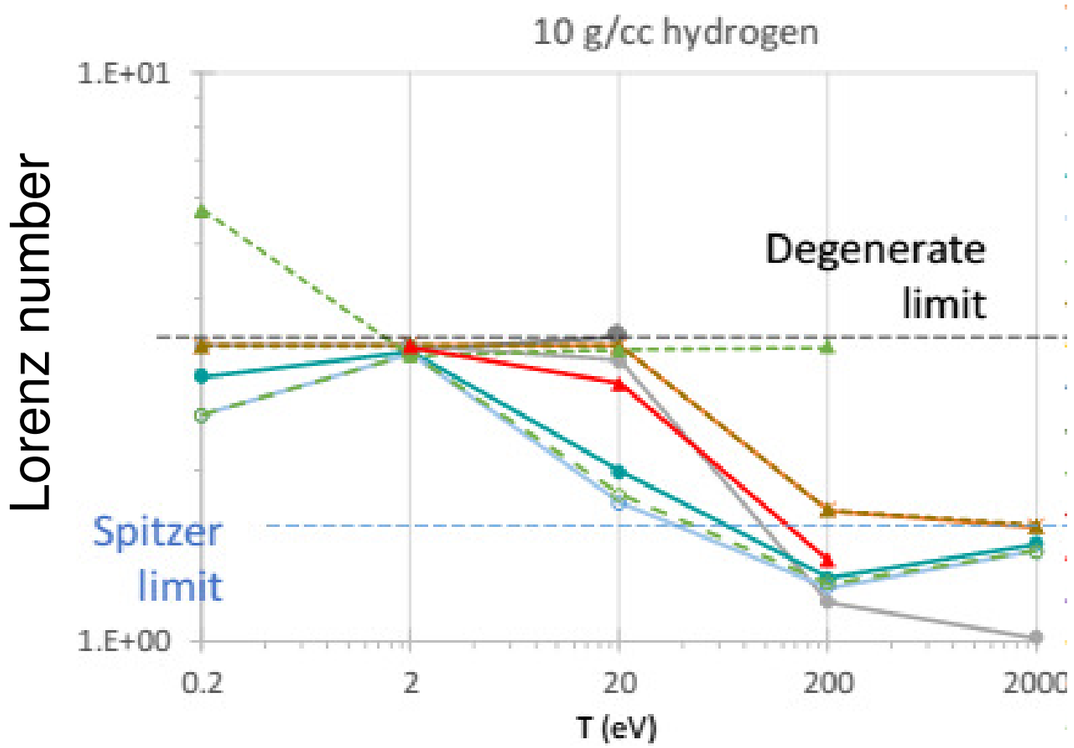

If you are interested in participating in the next workshop, planned for spring 2018 at LLNL, please contact Alex Zylstra, Paul Grabowski, Frank Graziani, Michael Murillo, or me!